PPPL--2430

DE87 013211

Effects of High Power Ion Bernstein Waves on a Tokamak Plasma

M. Ono, P. Beiersdorfer, R. Bell, S. Bernabei, A. Cavallo, A. Chmyga,†
S. Cohen, P. Colestock, G. Gammel,** G. J. Greene, J. Hosea, R. Kaita,
I. Lehrman,* G. Mazzitelli,** E. Mazzucato, D. McNeill, K. Sato,#
J. Stevens, J. Timberlake, J.R. Wilson, and A. Wouters

Princeton Plasma Physics Laboratory, Princeton University
P.O. Box 451, Princeton, NJ 08544, USA

ABSTRACT

Ion Bernstein wave heating (IBWH) has been investigated on PLT with up to 650 kW of rf power coupled to the plasma, exceeding the ohmic power of 550 kW. Plasma antenna loading of 2 Ω has been observed, resulting in 80-90% of the rf power being coupled to the plasma. An ion heating efficiency of $\Delta T_i(0)\bar{n}_e/P_{rf} = 6 \times 10^{13}$ eV cm^{-3}/kW, without high energy tail ions, has been observed up to the maximum rf power. The deuterium particle confinement during high power IBWH increases significantly (as much as 300%). Associated with it, a longer injected impurity confinement time, reduced drift wave turbulence activity, frequency shifts of drift wave turbulence, and development of a large negative edge potential were observed. The energy confinement time, however, shows some degradation from the ohmic value, which can be attributed to the enhanced radiation loss observed during IBWH. The ion heating and energy confinement time are relatively independent of plasma current.

†Kharkov Physico-Technical Institute, USSR
*Grummann Space Systems, Plainsboro, NJ
**Associazione EURATOM-ENEA, Frascati, Italy
#Institute of Plasma Physics, Nagoya, Japan

Plasma heating by directly launched ion Bernstein waves (IBWH) has been actively investigated in recent years[1-8] as an alternative to conventional heating methods. Due to their relatively short wavelength, the ion Bernstein waves can heat the bulk ion distributions even at relatively high harmonic frequencies.[1] The wave polarization and the relatively wide operating frequency range permit a flexible waveguide launcher design,[9-10] which is attractive even for the compact ignition device.[11]

In previous lower power tokamak IBWH experiments, various interesting heating regimes were identified. In JIPPT-II-U, a strong ion heating regime at 3/2 Ω_D and an electron heating regime at the Ω_H-minority resonance[3] were observed. On PLT, efficient heating regimes including 5 Ω_D, H-minority, ^{3}He-minority, and 3/2 Ω_D were observed.[12,13] The rf power for these experiments was 60-150 kW. The observed ion heating quality factor $\Delta T_i(0)\bar{n}_e/P_{rf}$ was about 3-6 × 10^{13} cm^{-3}/kW for these regimes. These initial experiments demonstrated that IBWH can heat bulk ions even at relatively high harmonics of the ion cyclotron frequency without producing a significant high energy ion tail population. IBWH can also interact nonlinearly with subharmonics of the ion cyclotron frequencies, giving rise to new heating scenarios.[2,6,7,13]

In this paper, we report results of the PLT high power IBWH experiments ($P_{rf} \gtrsim P_{oh}$), where plasma confinement issues could be tested.[14] It was of particular interest to study the confinement properties arising from bulk ion heating, as opposed to those from high-energy-ion-based heating such as fast wave ICRF and neutral beam heating.

In order to excite preferentially the ion Bernstein wave (as opposed to the fast wave) a B_θ-E_z type loop coupler was used.[2] The rf current for this antenna flows in the toroidal direction, whereas the fast wave antenna has its current flowing in the poloidal direction. The new high power IBWH antenna is

a 60-cm long and 5-cm wide simple loop antenna. The distance from the current strip to the back plate is 5 cm. The antenna is covered with MACOR cover plates. Between the MACOR and the plasma, there are two layers of stainless steel Faraday shields. The antenna is protected by graphite plates placed toroidally on both sides of the antenna. Two high power IBWH antennas were installed on PLT. With these antennas up to 800 kW of rf power could be applied to the antenna. The plasma loading for such an antenna was ~ 2 Ω, resulting in 80-90% coupling of the applied rf power to the plasma.[15] Overall antenna performance was similar to the PLT high power fast wave antenna.

IBWH at high power levels was performed in PLT circular limiter discharges with major and minor radii of 132 cm and 39 cm. The ^{3}He and 3/2 Ω_D heating regimes were investigated utilizing the PLT 30 MHz transmitters. Typical heating results are shown in Fig. 1(a), where a time evolution of the ion temperature is shown for 3/2 Ω_D heating at the 500 kW level in a deuterium plasma with $\bar{n}_e = 3 \times 10^{13}$ cm^{-3}. Three T_i diagnostic techniques, Doppler broadening (Ti XXI), charge exchange (Cx), and neutron emission, are in good general agreement within the uncertainties of each diagnostic. The charge-exchange velocity distribution is Maxwellian without any high energy tail ions up to the highest power level. The ion temperature profile as measured by the Doppler broadening of various ion lines is centrally peaked, similar to the ohmic profile [Fig. 1(b)]. In the 500-600 kW range, the central Doppler ion temperature reaches ≈ 2 keV, which exceeds the central TVTS (television Thomson scattering) electron temperature. The time evolution of the plasma density is shown in Fig. 2(a). The dashed curves are that of an ohmic case where the gas feed is programmed to yield a similar density evolution.

During IBWH, the particle confinement shows a significant improvement.[4] A clear example is shown in Fig. 2(a), where the plasma density increases by more than a factor of three. This occurs without active gas puffing and without increasing particle recycling, as indicated by a drop in the D_α emission. As shown in Fig. 2(b), the D_α emission near the antenna-limiter region (the main recycling region) during IBWH (solid curve) is significantly less than that in the programmed OH (dashed curve) case. This density rise during IBWH does not correlate with the impurity influx measured by various spectroscopic instruments, a Bremsstrahlung based "Z"-meter, and a scanning bolometer. Also, the large increase in neutron level (a factor of 500) shows that the incremental density is due mainly to deuterium. The density profiles during IBWH are similar to the simulated ohmic case as shown by Fig. 2(c). The density in the limiter scrape-off region is less for the IBWH case, suggesting a steeper density gradient in the plasma edge region.

Associated with this improvement in the particle confinement, a number of interesting phenomena were observed. During IBWH, the low energy neutral flux levels (at energies less than 1 keV) decrease significantly.[7] This drop may be related to the drop in the D_α emission. In order to further understand the particle transport processes during IBWH, a laser blow-off impurity injector was used to inject a very small amount of selenium. As shown by Fig. 3(a), the decay time of the Se XXV radiation increases by a factor of two from the ohmic level (from 50 msec to 100 msec). Since during the observation time, the central electron density and temperature are nearly constant for both cases, the selenium line behavior gives an indication of the central selenium confinement. Similar behavior was observed with a helium gas puff. By injecting a given amount of helium with a pre-programmed fast gas valve, the net density rise during IBWH is at least twice the level of the no rf case, again suggesting an improvement in the particle confinement time. This relatively similar confinement improvement for the low Z ions (hydrogen and helium) compared with the high Z ions (selenium) suggests non-neoclassical particle diffusion behavior.[16]

Another striking effect of IBWH is in the change of the low frequency turbulence activity in the plasma. A microwave scattering system[17] was used to investigate the turbulence in a half-radius region between the q=1 and q=3 surfaces, r ≈ 25 ± 10 cm. It is generally believed that the low frequency turbulence activity in this region plays an important role in the anomalous transport processes in tokamak plasmas.[18] In Fig. 3(b), the time evolutions of the scattering signals at 100 kHz for both the IBWH and simulated ohmic cases are shown. In this case, the scattered wave number is 6-8 cm^{-1}. One can see a significant drop in the turbulence level during IBWH as compared to the simulated ohmic case. In the inset, the frequency spectrum in each case is shown immediately after the end of rf (t = 710 msec). A frequency shift along with an amplitude reduction occurs during IBWH. Since the plasma density profiles are similar in both cases, one can rule out the possibility of a change in the scattering volume. From the frequency shift, one can infer a net increase of the poloidal rotational velocity of approximately 5×10^4 cm/sec in the electron diamagnetic drift direction. This drift velocity would correspond to an electric field of 15 volt/cm in the radially inward direction. It should be noted here that this clear reduction in the drift wave activity correlates well with the long impurity particle confinement. Measurements with an rf-shielded Langmuir probe in the plasma edge have shown the development, during IBWH, of a large floating potential which is negative with respect to the chamber wall [Fig. 3(c)]. This observation is again correlated with the appearance of a frequency shift in the turbulence spectrum. These observations are indeed similar to the results of recent limiter-bias experiments, where negative bias has produced improved particle confinement with a corresponding reduction in the low frequency turbulence activity.[19] One may also note that a general reduction of the turbulence activity was observed during the H-mode phase of the neutral-beam-heated PDX plasmas where the plasma density showed a similar rise.[20]

The mechanism for the negative potential produced during IBWH is not well understood. One possible mechanism for the negative charging of the plasma is the enhancement of the ion losses from the plasma as is believed to occur during counter injection of neutral beams.[21] This is not obvious for IBWH since we do not see a significant generation of high energy tail ions nor any evidence of an edge ion heating. Another possible mechanism is enhanced electron particle confinement, perhaps related to the reduction in the low frequency turbulence activity, which can also charge the plasma negative.

Plasma energy confinement during IBWH is of interest due to its bulk ion heating properties. The ion heating efficiency as shown in Fig. 4(a) is nearly linear up to a 650 kW level, with a heating quality factor of $\Delta T_i(0)$ $\bar{n}_e/P_{rf}$ = 6-7 × 10^{13} eV cm^{-3}/kW which is comparable to the best PLT ICRH heating efficiency.[22] It is interesting to note that both ^3He and 3/2 Ω_D heating have similar heating efficiencies. The toroidal magnetic field for 3/2 Ω_D heating is about 10% lower than the ^3He case and the 3/2 Ω_D regime, of course, requires no ^3He injection. In Fig. 1(b), the calculated ion temperature profiles, assuming an ohmic ion energy diffusion coefficient, are plotted as dashed curves and agree quite well with the measured profile. This provides an indication that no ion transport deterioration occurred during IBWH.[13] However, the global energy confinement shows a gradual degradation of confinement time with increased rf power as shown in Fig. 4(b). At 650 kW, the confinement time is about 40 msec at $\bar{n}_e$ = 4.5 × 10^{13} cm^{-3}, which is significantly below the ohmic value of 50-55 msec, but appears to be higher than the L-mode scaling time of ≈ 33 msec.[23] The IBWH confinement time actually increases with the plasma density, similar to the results on PLT with fast wave ICRF heating,[24] whereas neutral beam L-mode scaling tends to be relatively constant with density. The deviation from ohmic confinement can be attributed to an increase in the electron loss channel, which is mainly due to the increased radiation loss. The radiation profile during IBWH as measured by a scanning bolometer shows a more centrally peaked profile, with the total radiated power increasing by a factor of three. However, the electron diffusivity, which takes this radiation loss into account, remains ohmic-like.

To investigate the scaling of energy confinement with plasma current, the current was varied between 200 kA (q_{edge} = 10) to 630 kA (q_{edge} = 3) with a constant rf power level of 250 kW. We find that for a given rf power, the ion temperature increase remains constant down to the lowest current of 200 kA. The normalized confinement time, $\tau_E/\bar{n}_e$, also remains constant as can be seen in Fig. 4(c). This behavior may be due to the bulk ion heating characteristic of IBWH that fast ion losses are negligible, even for the low current case.

During IBWH, an increase in the influx of metallic impurities (predominantly iron) was observed. This high-Z impurity influx, together with the longer particle confinement, can result in non-negligible central radiation losses during high power (high density) IBWH. Therefore, it is quite important in a successful high power IBWH experiment to reduce the iron influx level as much as possible. In order to understand the source of the iron impurities, the Faraday shields of one of the antennas were coated with a 20-μ-thick carbon film.[25] For the same rf power level, the antenna with the carbon-coated outer shields produced half as much iron influx (and half as much central bolometric radiation) as the uncoated antenna. When the Faraday shields were fully coated (inner and outer), the iron level decreased by another factor of two. The ion heating efficiency and the density rise, however, remained relatively independent of the coating. This indicates that most of the iron influx originated from the Faraday shields, making the Faraday shield design one of the most important elements of future IBWH antenna development. This finding also makes an IBWH waveguide launcher an even more interesting prospect for future IBWH experiments.

In conclusion, efficient ion heating by IBWH was observed in the ^3He and $3/2\ \Omega_D$ regimes up to the highest power level (P_{rf} = 650 kW). With the application of IBWH, significant improvement in the deuterium particle confinement time was observed. Associated with this improvement, longer confinement time of injected selenium and helium, reduced low frequency turbulence, and development of a large negative floating potential were observed. The global plasma energy confinement time at the highest power levels showed some degradation from the ohmic level, which was attributed to an increase in radiative losses. The ion heating and the energy confinement remained relatively constant as the plasma current varied. The ion energy distribution remained Maxwellian for the entire power range. Finally, it is interesting to note that overall, IBWH-produced plasmas have many similarities with H-mode plasmas. In view of these results, it is now important to investigate IBWH in a diverted plasma, as well as in conjunction with strong neutral beam heating.

Acknowledgments

The authors appreciated the support and encouragement given to the experiment by K. Bol, T.H. Stix, P. Rutherford, and H. Furth. One of the authors (M.O.) also appreciated discussions with Dr. M. Okamoto concerning plasma transport.

This work supported by U.S. Department of Energy Contract No. DE-AC02-76-CHO-3073.

References

1 M. Ono, G.A. Wurden, and K.L. Wong, Phys. Rev. Lett 52, 37 (1984).

2 M. Ono and T. Watari et al., Phys. Rev. Lett. 54, 2339 (1985).

3 T. Watari, "Applications of RF Waves to Tokamak Plasmas," Varenna, Italy, Sept. 1985.

4 J.C. Hosea et al., Plasma Physics and Controlled Fusion 28, 1241 (1986).

5 J.R. Wilson et al., J. Nucl. Matt. 145-146, (Feb. 1987).

6 H. Abe et al., Phys. Rev. Lett. 53, 1153 (1984).

7 M. Porkolab et al., Phys. Rev. Lett. 54, 434 (1985).

8 M. Porkolab et al., 11th Conference on Plasma Physics and Controlled Nuclear Fusion Research,Kyoto (1986), F-II-2.

9 Puri, Phys. Fluids 22, 1716 (1979).

10 M. Ono et al., 8th Conference on Plasma Physics and Controlled Nuclear Fusion Research, Brussels (1980), T-I-2(B).

11 J. Schmidt et al., 11th Conference on Plasma Physics and Controlled Nuclear Fusion Research, Kyoto (1986) H-I-2.

12 J.R. Wilson, AIP Conference Proceedings of Sixth Topical Conference on RF Plasma Heating, Callaway Gardens, Georgia, 1985, p. 8.

13 M. Ono, AIP Conference Proceedings of Sixth Topical Conference on RF Plasma Heating, Callaway Gardens, Georgia, 1985, p. 83.

14 M. Ono et al., 11th Conference on Plasma Physics and Controlled Nuclear Fusion Research, Kyoto, (1986), F-I-3.

15 G. J. Greene et al., Bull. Am. Phys. Soc. 31, 1467 (1986).

16 R.C. Isler, Nucl. Fusion 24, 1599 (1984).

17 E. Mazzucato, Phys. Fluids 21, 1063 (1978); Phys. Rev. Lett. 48, 1828 (1982).

[18] P.C. Liewer, Nucl. Fusion 25, 543 (1985).

[19] P.E. Phillips et al., J. Nucl. Mater. 145-146 (1987).

[20] T. Crowley and E. Mazzucato, Nucl. Fusion 25, 507 (1985).

[21] R. Kaita et al., Nucl. Fusion 25, 939 (1985).

[22] J. Hosea et al., 8th Conference on Plasma Physics and Controlled Nuclear Fusion Research, Brussels, (1980), D-5-1.

[23] S.M. Kaye, Phys. Fluids 28, 2327 (1985).

[24] P. Colestock et al., Bull. Am. Phys. Soc. 30, 1445 (1985).

[25] J. Timberlake et al., Bull. Am. Phys. Soc. 31, 1467 (1986).

Figure Captions

Fig. 1 Ion Heating. (a) A typical time evolution of ion temperature. P_{rf} = 500 kW, F = 30 MHz, B_o = 29 kG, 3/2 Ω_D, I_p = 500 kA, P_{OH} = 550 kW, and $\bar{n}_e = 3.0 \times cm^{-3}$. Other parameters are shown in Figs. 1(b) and 2. (b) Temperature profiles at t = 600 msec. Circles are the measured Doppler ion temperatures. The solid curve is the measured TVTS electron temperature profile. The dashed curves are ion temperature profiles calculated assuming an ohmic ion transport coefficient.

Fig. 2 (a) Density time evolution for IBWH case (solid curve) shown in Fig. 1 and ohmic case (dashed curve), in which the gas puffing was used to simulate the density rise of the IBWH case. (b) Time evolution of D_α emission for IBWH and simulated ohmic cases taken near the antenna-limiter region. (c) Density profiles at t = 600 msec for IBWH and a simulated ohmic case shown in Fig. 2(a). (d) Corresponding electron temperature profiles.

Fig. 3 (a) Time evolution of the selenium XXV resonance line intensity for IBWH and a simulated ohmic case. The selenium was injected at t = 550 msec. (b) Time evolution of low frequency turbulence level at 100 kHz for the two cases. k(scatt) = 6-8 cm^{-1} at r = 25 ± 10 cm. Insert-Frequency spectrum at t = 710 msec for the two cases. (c) Time evolution of the plasma edge floating potential.

Fig. 4 (a) Ion heating as a function of rf power for ^{3}He-minority (B_o = 32 kG, ≈ 10% ^{3}He) and 3/2 Ω_D(B_o = 29 kG, 0% ^{3}He) regimes. (b) Global energy confinement time as a function of the plasma line averaged density. The circles are the measured ohmic confinement time. The solid dots are the measured IBWH values. The corresponding injected rf power is shown in parentheses. The triangles are the values calculated from the L-mode scaling at comparable auxiliary heating power. (c) Normalized global confinement time as a function of plama current for a fixed rf power, P_{rf} = 250 kW (solid dots). The circles are the rf to ohmic power ratios.

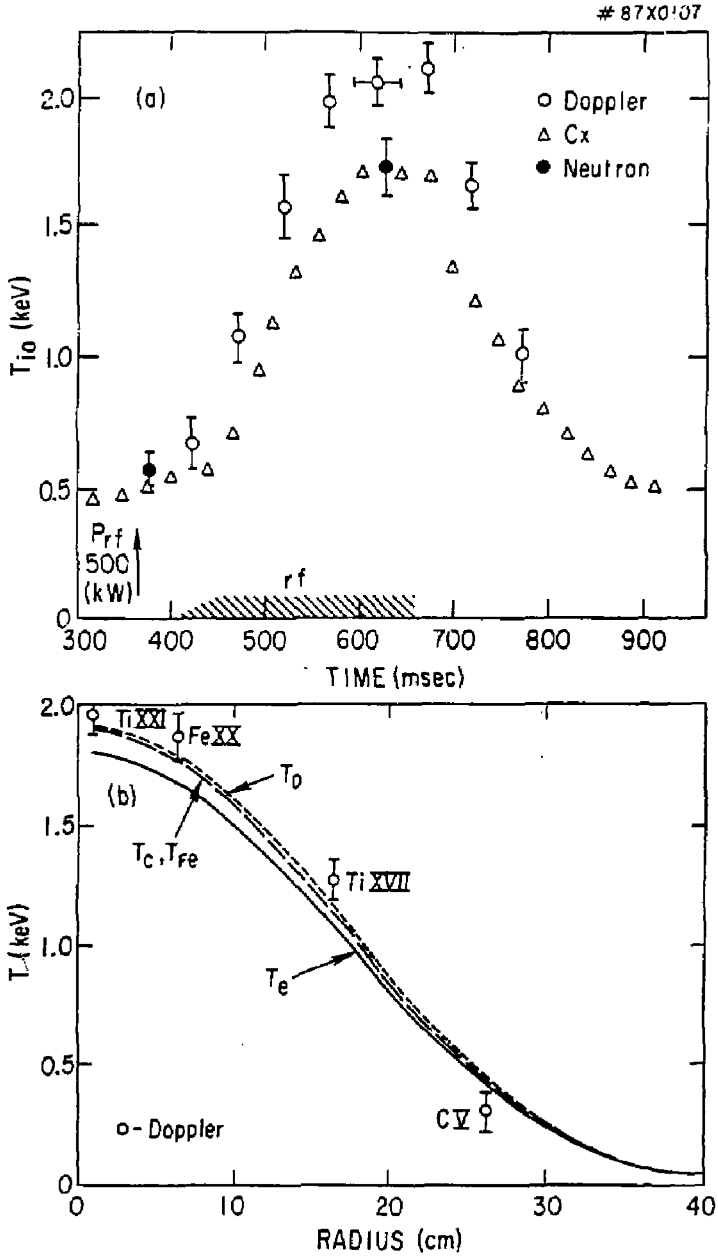

87X0107
(a)
Doppler
Cx
Neutron
T_{io} (keV)
P_{rf} 500 (kW)
rf
TIME (msec)
(b)
Ti XXI
Fe XX
T_D
T_C, T_{Fe}
Ti XVII
T_e
C V
o- Doppler
T (keV)
RADIUS (cm)

Fig. 1

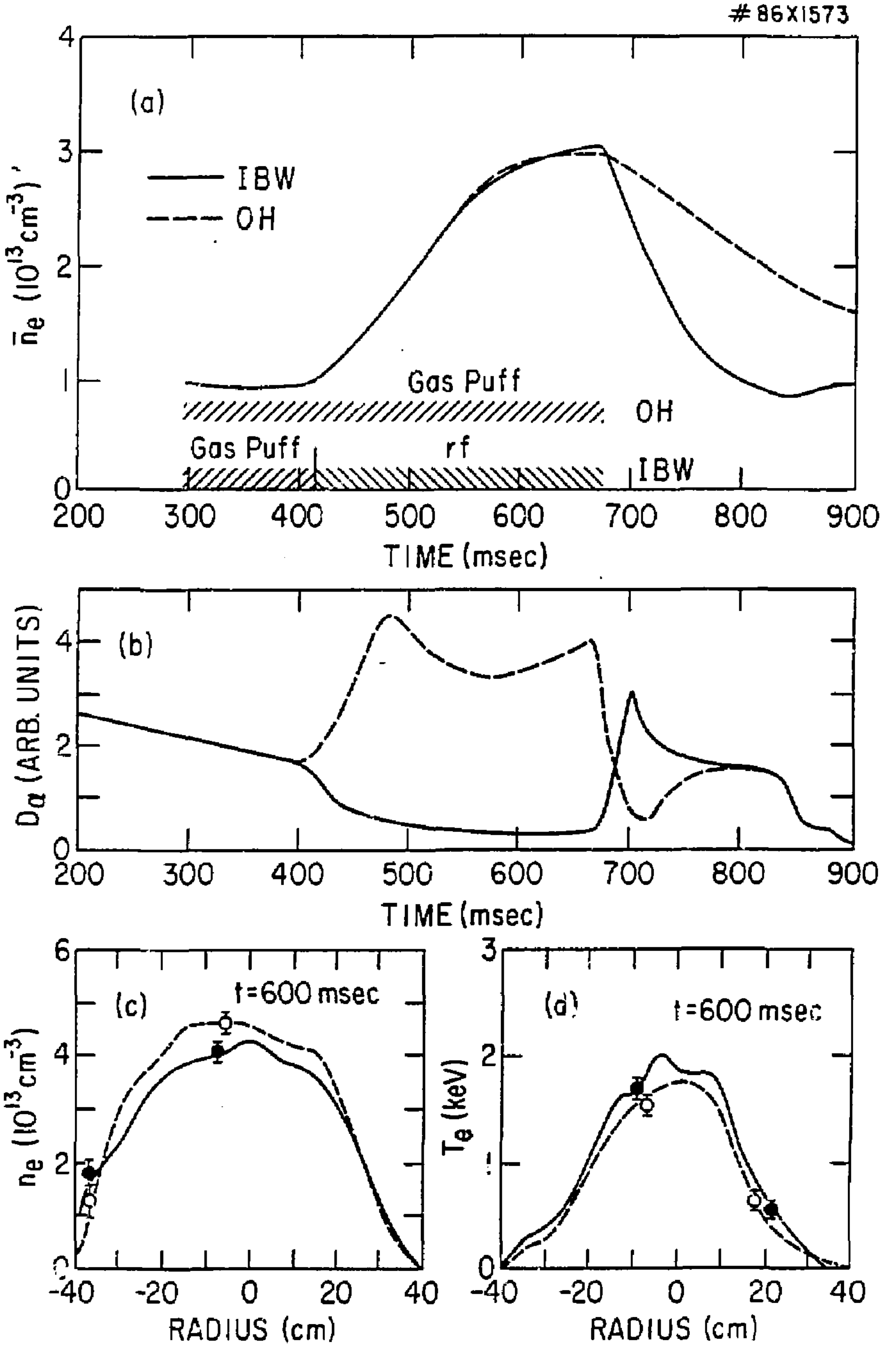
#86X1573
(a)
IBW
OH
$\bar{n}_e$ (10^{13}cm^{-3})
Gas Puff
OH
Gas Puff
rf
IBW
TIME (msec)
(b)
D_α (ARB. UNITS)
TIME (msec)
(c)
t=600 msec
n_e (10^{13}cm^{-3})
RADIUS (cm)
(d)
t=600 msec
T_e (keV)
RADIUS (cm)

Fig. 2

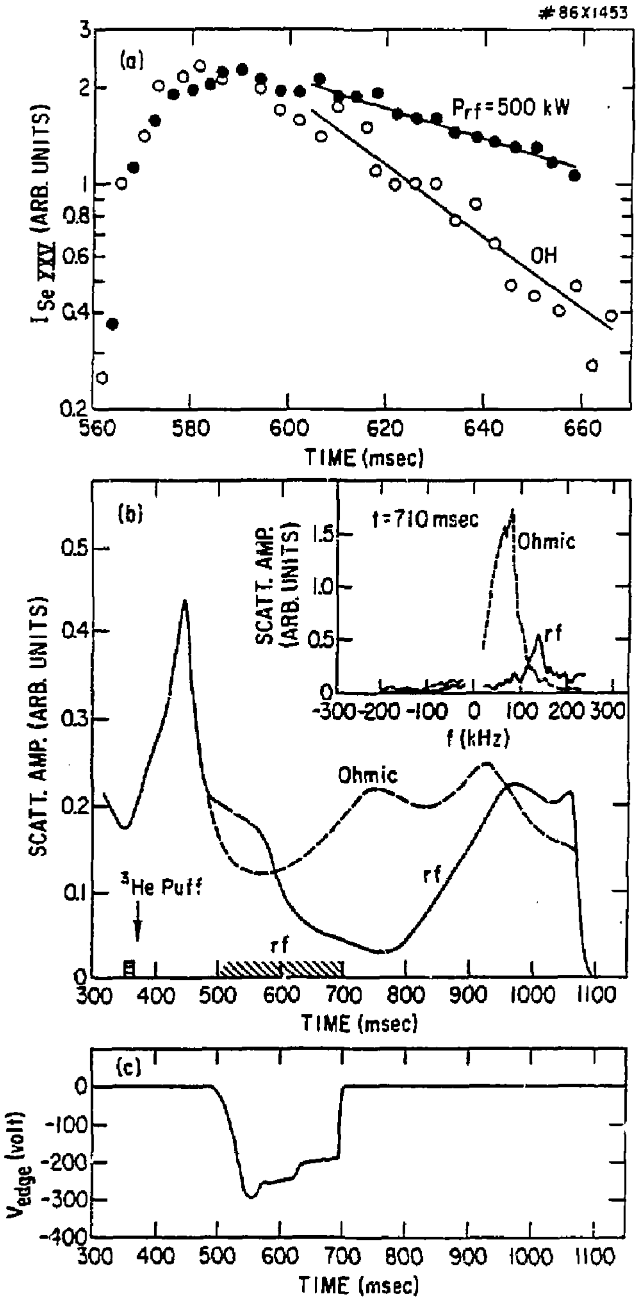

#86X1453
(a)
P_{rf}=500 kW
OH
$I_{Se\ XXV}$ (ARB. UNITS)
TIME (msec)
(b)
t=710 msec
Ohmic
rf
SCATT. AMP. (ARB. UNITS)
f (kHz)
Ohmic
rf
^{3}He Puff
rf
SCATT. AMP. (ARB. UNITS)
TIME (msec)
(c)
V_{edge} (volt)
TIME (msec)

Fig. 3

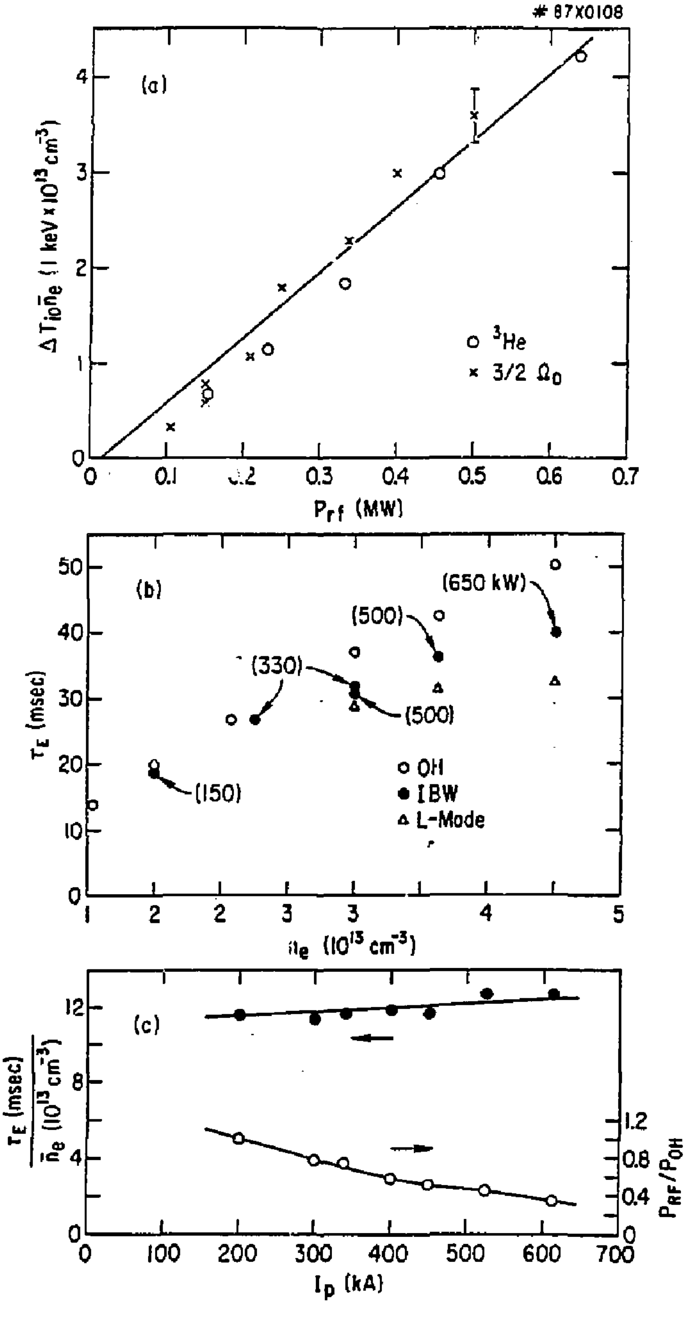

87X0108
(a)
ΔT_i0 n̄_e (1 keV × 10^13 cm^-3)
P_rf (MW)
³He
3/2 Ω_D
0
0.1
0.2
0.3
0.4
0.5
0.6
0.7
1
2
3
4
(b)
τ_E (msec)
n̄_e (10^13 cm^-3)
(650 kW)
(500)
(330)
(500)
(150)
OH
IBW
L-Mode
0
10
20
30
40
50
1
2
3
4
5
(c)
τ_E (msec) / n̄_e (10^13 cm^-3)
P_RF / P_OH
I_p (kA)
0
4
8
12
0.4
0.8
1.2
100
200
300
400
500
600
700

Fig. 4

EXTERNAL DISTRIBUTION IN ADDITION TO UC-20

Dr. Frank J. Paoloni, Univ of Wollongong, AUSTRALIA
Prof. M.H. Brennan, Univ Sydney, AUSTRALIA
Plasma Research Lab., Australian Nat. Univ., AUSTRALIA
Prof. I.R. Jones, Flinders Univ., AUSTRALIA
Prof. F. Cap, Inst Theo Phys, AUSTRIA
Prof. M. Heindler, Institut fur Theoretische Physik, AUSTRIA
M. Goossens, Astronomisch Instituut, BELGIUM
Ecole Royale Militaire, Lab de Phys Plasmas, BELGIUM
Com. of European, Dg XII Fusion Prog, BELGIUM
Prof. R. Boucique, Laboratorium voor Natuurkunde, BELGIUM
Dr. P.H. Sakanaka, Univ Estadual, BRAZIL
Instituto De Pesquisas Espaciasi-INPE, BRAZIL
Library, Atomic Energy of Canada Limited, CANADA
Dr. M.P. Bachynski, MPB Technologies, Inc., CANADA
Dr. H.M. Skarsgard, Univ of Saskatchewan, CANADA
Dr. H. Barnard, University of British Columbia, CANADA
Prof. J. Teichmann, Univ. of Montreal, CANADA
Prof. S.R. Sreenivasan, University of Calgary, CANADA
Prof. Tudor W. Johnston, INRS-Energie, CANADA
Dr. C.R. James, Univ. of Alberta, CANADA
Dr. Peter Lukac, Komenskeho Univ, CZECHOSLOVAKIA
The Librarian, Culham Laboratory, ENGLAND
Mrs. S.A. Hutchinson, JET Library, ENGLAND
C. Mouttet, Lab. de Physique des Milieux Ionises, FRANCE
J. Radet, CEN/CADARACHE - Bat 506, FRANCE
Dr. Tom Mual, Academy Bibliographic, HONG KONG
Preprint Library, Cent Res Inst Phys, HUNGARY
Dr. B. Dasgupta, Saha Inst, INDIA
Dr. R.K. Chhajlani, Vikram Univ. INDIA
Dr. P. Kaw, Institute for Plasma Research, INDIA
Dr. Phillip Rosenau, Israel Inst Tech, ISRAEL
Prof. S. Cuperman, Tel Aviv University, ISRAEL
Librarian, Int'l Ctr Theo Phys, ITALY
Prof. G. Rostagni, Univ Di Padova, ITALY
Miss Clelia De Palo, Assoc EURATOM-ENEA, ITALY
Biblioteca, del CNR EURATOM, ITALY
Dr. H. Yamato, Toshiba Res & Dev, JAPAN
Prof. I. Kawakami, Atomic Energy Res. Institute, JAPAN
Prof. Kyoji Nishikawa, Univ of Hiroshima, JAPAN
Direc. Dept. Lg. Tokamak Res. JAERI, JAPAN
Prof. Satoshi Itoh, Kyushu University, JAPAN
Research Info Center, Nagoya University, JAPAN
Prof. S. Tanaka, Kyoto University, JAPAN
Library, Kyoto University, JAPAN
Prof. Nobuyuki Inoue, University of Tokyo, JAPAN
S. Mori, JAERI, JAPAN
M.H. Kim, Korea Advanced Energy Research Institute, KOREA
Prof. D.I. Choi, Adv. Inst Sci & Tech, KOREA
Prof. B.S. Liley, University of Waikato, NEW ZEALAND
Institute of Plasma Physics, PEOPLE'S REPUBLIC OF CHINA
Librarian, Institute of Phys., PEOPLE'S REPUBLIC OF CHINA
Library, Tsing Hua University, PEOPLE'S REPUBLIC OF CHINA
Z. Li, Southwest Inst. Physics, PEOPLE'S REPUBLIC OF CHINA
Prof. J.A.C. Cabral, Inst Superior Tecn, PORTUGAL
Dr. Octavian Petrus, AL I CUZA University, ROMANIA
Dr. Johan de Villiers, Plasma Physics, AEC, SO AFRICA
Prof. M.A. Hellberg, University of Natal, SO AFRICA
Fusion Div. Library, JEN, SPAIN
Dr. Lennart Stenflo, University of UMEA, SWEDEN
Library, Royal Inst Tech, SWEDEN
Prof. Hans Wilhelmson, Chalmers Univ Tech, SWEDEN
Centre Phys des Plasmas, Ecole Polytech Fed, SWITZERLAND
Bibliotheek, Fom-Inst Voor Plasma-Fysica, THE NETHERLANDS
Dr. D.D. Ryutov, Siberian Acad Sci, USSR
Dr. G.A. Eliseev, Kurchatov Institute, USSR
Dr. V.A. Glukhikh, Inst Electro-Physical, USSR
Dr. V.T. Tolok, Inst. Phys. Tech. USSR
Dr. L.M. Kovrizhnykh, Institute Gen. Physics, USSR
Prof. T.J.M. Boyd, Univ College N Wales, WALES
Nuclear Res. Establishment, Julich Ltd., W. GERMANY
Bibliothek, Inst. Fur Plasmaforschung, W. GERMANY
Dr. K. Schindler, Ruhr Universitat, W. GERMANY
ASDEX Reading Rm, IPP/Max-Planck-Institut fur Plasmaphysik, W. GERMANY
Librarian, Max-Planck Institut, W. GERMANY
Prof. R.K. Janev, Inst Phys, YUGOSLAVIA